Journal of Biotechnology 328 (2021) 12–22

Contents lists available at ScienceDirect

Journal of Biotechnology

journal homepage: www.elsevier.com/locate/jbiotec

Effect of *lhcsr* gene dosage on oxidative stress and light use efficiency by *Chlamydomonas reinhardtii* cultures

Simone Barera, Luca Dall'Osto, Roberto Bassi *

Dipartimento di Biotecnologie, Università di Verona, Strada Le Grazie 15, 37134, Verona, Italy

ARTICLE INFO

Keywords:
Photosynthesis
Algae
Cell growth
Photoprotection
NPQ
Biomass

ABSTRACT

Unicellular green algae, a promising source for renewable biofuels, produce lipid-rich biomass from light and CO_2. Productivity in photo-bioreactors is affected by inhomogeneous light distribution from high cell pigment causing heat dissipation of light energy absorbed in excess and shading of the deep layers. Contrasting reports have been published on the relation between photoprotective energy dissipation and productivity. Here, we have re-investigated the relation between energy quenching (qE) activity, photodamage and light use efficiency by comparing WT and two *Chlamydomonas reinhardtii* strains differing for their complement in LHCSR proteins, which catalyse dissipation of excitation energy in excess (qE). Strains were analysed for ROS production, protein composition, rate of photodamage and productivity assessed under wide light and CO_2 conditions.

The strain lacking LHCSR1 and knocked down in LHCSR3, thus depleted in qE, produced O_2 at significantly higher rate under high light, accompanied by enhanced singlet oxygen release and PSII photodamage. However, biomass productivity of WT was delayed in respect for mutant strains under intermittent light conditions only, implying that PSII activity was not the limiting factor under excess light. Contrary to previous proposals, domestication of *Chlamydomonas* for carbon assimilation rate in photo-bioreactors by down-regulation of photoprotective energy dissipation was ineffective in increasing algal biomass productivity.

1. Introduction

The massive burning of fossil fuels makes the search for carbon-neutral fuels solutions urgent. Liquid fuels derived from unicellular algae represent a renewable alternative to fossil fuels as a source of sustainable energy for. Mass culture of microalgae in photobioreactors (PBRs) is a promising source of lipid-rich biomass for biofuel production on an industrial scale, due to the high productivity and lipid-content, far exceeding the best crops (Scott et al., 2010) (Benedetti et al., 2018) (Borowitzka e Moheimani, 2013). Despite microalgae and land plants share the same basic function of photosynthetic reactions (Nelson e Ben-Shem, 2004); the simpler structure of unicellular algae lacking roots and other non-photosynthetic organs, makes microalgae more efficient in converting solar energy into biomass. Additional advantages of growing microalgae are the lack of competition with food crops for arable soils and the high level of lipids, up to over 50% of their dry biomass (Rodolfi et al., 2009). Production of biomass from microalgae, however, still suffers from limitations, undermining cost effectiveness. These include the investment for PBRs construction and management, water pumping and mixing, axenic practices for preventing contamination of monocultures, harvesting biomass and lipid extraction (Benedetti et al., 2018) (Vecchi et al., 2020). Physiological limitations also contribute, such as low light use efficiency under high irradiance due to energy dissipation. The maximal theoretical efficiency of photosynthetically active radiation (PAR, 400−700 nm) solar energy conversion into biomass is about 27% (Weyer et al., 2010). However, such values are only observed at low light intensity in laboratory-scale growth trials, while efficiency drops below 6% in outdoor cultures at full sunlight (Zhu et al., 2010). Physiological limits in biomass yield can be ascribed to a number of factors (Stephenson et al., 2011), including (i) light saturation effect yielding into photoprotective energy dissipation, (ii) inhomogeneous light distribution within a mass culture with respiratory loss

Abbreviations: Car, carotenoids; Chl, chlorophylls; DCMU, 3-(3,4-dichlorophenyl)-1,1-dimethylurea; DW, dry weight; EL, excess light; Fv/Fm, maximal quantum yield of PSII; LHCI/II, light-harvesting complex of PSI/II; NPQ, non-photochemical quenching; Pmax, maximal photosynthetic rate; PAR, photosynthetic active radiation; PBR, photobioreactor; PSI/II, photosystem I/II; ROS, reactive oxygen species; WT, wild-type; 1Chl*, singlet excited state of Chl; 3Chl*, triplet excited state of Chl; 1O2, singlet oxygen.

* Corresponding author.
E-mail addresses: simone.barera@univr.it (S. Barera), luca.dallosto@univr.it (L. Dall'Osto), roberto.bassi@univr.it (R. Bassi).

https://doi.org/10.1016/j.jbiotec.2020.12.023
Received 31 August 2020; Received in revised form 27 November 2020; Accepted 31 December 2020
Available online 9 January 2021

in deep layers, and (iii) photoinhibition of high light exposed surface cell layers.

The light absorption by photosynthetic pigments causes light saturation effect, with photon harvesting to diverge from photosynthetic assimilation rate (Li et al., 2009) when high light intensity causes saturation of downstream biochemical reactions (P_{max}), with the balance being dissipated into heat (Ruban et al., 2012). At even higher fluency, net assimilation decreases due to oxidative photoinhibition (Barber, 2009). Additional energy loss derives from the inhomogeneous light distribution in the algal culture. The high Chl content per cell is aimed to maximize the photon capture in limiting light and is due to large arrays of antenna complexes (Light-harvesting complexes, LHCs), binding chlorophylls (Chl) and carotenoid (Car) in *quasi-molar* concentration which enhance exciton supply to reaction centres where photochemical reactions are catalysed (Van Amerongen e Croce, 2013). However, large antenna systems do not enhance overall productivity in a PBR because the higher optical density of algal cells makes light gradient even steeper, leaving underlying cell layers below compensation point thus, causing energy loss from respiration (Formighieri et al., 2012) (Cazzaniga et al., 2014). Upon sustained over-excitation experienced by cells in surface layers, an increase Chl singlet excited states (^{1}Chl*) and intersystem crossing to the Chl triplet state (^{3}Chl*) occur. Chl excited states react with molecular oxygen (O_2) yielding singlet oxygen ($^1O_2$), hence photoinhibition of PSII highly susceptible to light damage (Cazzaniga et al., 2014) (Li et al., 2018). In PBRs algal cells rapidly shift between layers with low *versus* high irradiance due to mixing, which impairs the light acclimation capacity of their photosynthetic apparatus (Dall'Osto et al., 2019) and activates excess energy dissipation. Engineering excess energy dissipation has been reported to be an effective strategy for enhancing biomass productivity in plants (Kromdijk et al., 2016) and in unicellular algae (Perozeni et al., 2018). Conversely, some reports showed that light use efficiency of *npq4* genotypes, with strongly reduced NPQ (Peers et al., 2009a) was unaffected, suggesting productivity of low NPQ strains might be dependent on growth light intensity and not by photoinhibition. We therefore analysed in detail the relation between NPQ activity, singlet oxygen production, photoinhibition and biomass accumulation in *Chlamydomonas reinhardtii* strains differing for their content in LHCSR proteins.

2. Results

2.1. Light-response of O_2 evolution and stoichiometry of thylakoids proteins

The dependence of O_2 evolution on light intensity was measured (Fig. 1A). In the dark, respiration rate was the same for the three genotypes growth in control light conditions (50 µmol photons m^{-2} s^{-1}). The compensation point was determined at approx. 10 µmol photons m^{-2} s^{-1} for all strains. With increasing light intensity, however, the saturating effect was faster in WT and *npq4*, with *npq4 lhcsr1* evolving significantly higher O_2 than both WT and *npq4* at light intensity above 1000 µmol photons m^{-2} s^{-1}. The accumulation of major protein complexes in cultures grown under low light (50 µmol photons m^{-2} s^{-1}s) was investigated by immunoblotting with specific antibodies targeting subunits PsaA, CP47, LHCII, Cytochrome *f* and the β subunit of chloroplastic ATPase (Fig. 1B), representative of PSI, PSII, Cyt-b_6f and ATPase supercomplexes respectively. Densitometric analysis was performed on titrated membranes and data were reported in Fig. 1C: the pattern of protein subunits was very similar in WT and *npq* mutants except the level of PsaA subunit which was higher in *npq4 lhcsr1* mutant compared to WT and *npq4*. RuBisCO accumulation showed a similar pattern in all genotypes, suggesting that downstream reactions were not the limiting step for biomass accumulation in these strains.

2.2. Pigment composition and organization into complexes with increasing growth light intensity

To investigate the effect of different light intensities on thylakoid composition in WT *versus*. *npq* mutants, we analysed cell pigments (Table 1) and thylakoid membranes (Fig. 2) isolated from cells grown under different light regimes: 50 (LL, low light), 400 (ML, medium light) and 1000 (HL, high light) µmol photons m^{-2} s^{-1}. Acclimation to different irradiance conditions is well known to induce variations in pigment content and relative composition in higher plants. An increase in the Chl *a/b* ratios was observed in all genotypes with increasing light intensity, being significantly higher in both WT and *npq4* genotypes than *npq4 lhcsr1* (Table 1). Because Chl *b* is a component of light-harvesting antenna systems of both PSI and PSII, this result suggests that acclimation to different light conditions does influence photosynthetic antenna sizes in *C. reinhardtii*. To determine whether the capacity of the antenna system to harvest energy was differentially affected by the mutations, the functional antenna size of PSII was quantified on cell suspensions in the presence of DCMU, by estimating the rise time of Chl *a* fluorescence. The $T_{2/3}$ of the Chl fluorescence rise, which is inversely related to the functional antenna size of PSII (Malkin et al., 1981) was reduced to the same extent in all genotypes: by ~ 37% in ML, by ~42% in HL *versus*. LL (Table 1).

Moreover, a higher amount of carotenoids per Chl was observed in all genotypes in ML and HL conditions with respect for the LL cultures. Chlorophyll content per cell was inversely proportional to irradiance during growth, being reduced to the same extent in all genotypes at increasing irradiances, suggesting a general reduction in photosynthetic pigment proteins (Table 1).

Pigment-protein complexes were separated by non-denaturing Deriphat-PAGE following solubilization with dodecyl-α-D-maltoside. All three strains showed similar electrophoretic profiles with five major

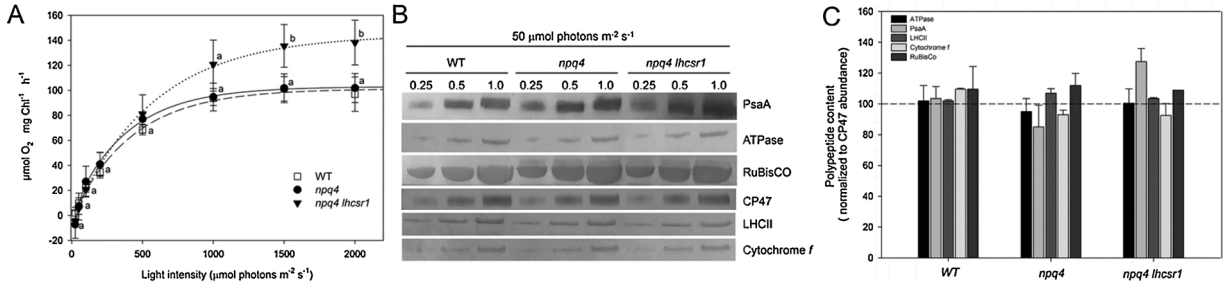

Fig. 1. Functional properties and composition of the photosynthetic apparatus. (A) Light-saturation curves of photosynthesis. Data are expressed as mean ± SD, n = 3 biologically independent samples. Values marked with different letters are significantly different from each other at the same light intensity (ANOVA followed by Tukey's post test at a significant level of $P < 0.05$). (B) Immunotitration performed on proteins extract from WT and *npq* mutants using antibodies directed against individual gene products: CP47, PsaA, Cytochrome *f*, ATPase β-subunit, LHCII and RuBisCO. The amount of Chls loaded for each lane is shown. (C) The abundance of each subunit was analysed by densitometry, normalized to the CP47 signal and expressed as a percentage of the corresponding WT content. Each genotype was growth in control conditions (50 µmol photons m^{-2} s^{-1}, 25 °C). Data are expressed as mean ± SD, n = 3.

Table 1
Pigment content and PSII functional antenna size of WT and npq mutants. Parameters were measured on dark-adapted cell suspension of *WT*, *npq4* and *npq4 lhcsr1* strains, upon 7 days of photoautotrophic growth under different light conditions. Data are expressed as mean ± SD, n = 3. For each parameter measured, significantly different values among genotypes at a given light regime (ANOVA test, $p < 0.05$) are marked with different letters.

	Light intensity (µmol photons m^{-2} s^{-1})	WT	*npq4*	*npq4 lhcsr1*
Chl a / b	50, continuous	202 ± 002[a]	195 ± 002[b]	211 ± 001[c]
	400, continuous	219 ± 004[a]	222 ± 001[a]	213 ± 006[a]
	1000, continuous	230 ± 001[a]	224 ± 001[b]	220 ± 002[c]
	400, 5 min light / 5 min dark	198 ± 001[a]	210 ± 001[b]	200 ± 001[a]
	800, 5 min light / 5 min dark	207 ± 001[a]	206 ± 003[a]	209 ± 005[a]
Chl / Car	50, continuous	101 ± 003[a]	115 ± 001[b]	109 ± 008[a,b]
	400, continuous	080 ± 012[a]	093 ± 008[a]	076 ± 007[a]
	1000, continuous	058 ± 006[a]	067 ± 006[a]	060 ± 001[a]
	400, 5 min light / 5 min dark	053 ± 011[a]	067 ± 007[a]	049 ± 005[a]
	800, 5 min light / 5 min dark	062 ± 006[a]	067 ± 008[a]	059 ± 003[a]
pg Chl $cell^{-1}$	50, continuous	259 ± 007[a]	296 ± 001[b]	281 ± 022[a,b]
	400, continuous	206 ± 030[a]	239 ± 021[a]	196 ± 018[a]
	1000, continuous	150 ± 015[a]	172 ± 016[a]	156 ± 001[a]
	400, 5 min light / 5 min dark	136 ± 027[a]	169 ± 017[a]	126 ± 014[a]
	800, 5 min light / 5 min dark	159 ± 016[a]	139 ± 008[a]	151 ± 005[a]
PSII antenna size ($t_{2/3}^{-1} \cdot 10^3$, ms^{-1})	50, continuous	4316 ± 072[a]	4073 ± 332[a]	4347 ± 199[a]
	400, continuous	2770 ± 040[a]	2603 ± 064[a]	2707 ± 096[a]
	1000, continuous	2463 ± 086[a]	2545 ± 102[a]	2485 ± 117[a]
	400, 5 min light / 5 min dark	4240 ± 126[a]	4156 ± 070[a]	4280 ± 075[a]
	800, 5 min light / 5 min dark	2965 ± 238[a]	2980 ± 041[a]	2989 ± 233[a]

green bands resolved, as shown in Fig. 2. However, Deriphat-PAGE showed some differences in the intensity of the bands, in the *npq* mutants profiles *versus.* WT: the level of monomeric PSII core complexes was reduced while dimeric PSII bands increased in the mutants *versus* WT, particularly at high light. The abundance PSI-LHCI high molecular mass was higher in *npq* mutants in respect for WT under all light treatments, particularly in *npq4 lhcsr1* mutant. This high PSI-LHCI feature was also evident at higher light conditions, and to a lesser extent in *npq4*, suggesting enhancement of PSI was part of the response to light with decreasing LHCSR.

2.3. Lack of LHCSR proteins enhances $^1O_2$ release

To investigate the relation between productivity, energy dissipation, $^1O_2$ release and photoinhibition, we proceeded to characterize algal cells grown at very different light intensities, *i.e.* 50 (LL), 400 (ML), and 1000 (HL) µmol photons m^{-2} s^{-1}, 25 °C, as for their NPQ activity.

Accumulation of LHCSR proteins and NPQ activity. The accumulation of LHCSR proteins strains was assessed by immunoblot analysis upon growth at increasing irradiances, 25 °C for 6 days in order to obtain full expression of both LHCSR1 and LHCSR3 proteins (Peers et al., 2009a). Immunoblot (Fig. 3 showed three anti-LHCSR reactive bands corresponding to LHCSR1, LHCSR3 and LHCSR3-P (phosphorylated form) (Bonente et al., 2011) which were all present in WT strain. The *npq4* strain only showed the LHCSR1 protein and the LHCSR3-P band. No anti-LHCSR-reactive bands were present in *npq4 lhcsr1*. The kinetics of NPQ activity were measured as induced by exposure of cell suspensions to 1600 µmol photons m^{-2} s^{-1} white actinic light. Before measurements, cells grown at different irradiances for 8 days were dark-adapted for 25 min. Through measurements, a background far-red light of 10 µmol photons m^{-2} s^{-1} was used in order to maintain state I conditions during recovery. For all growth conditions, the amplitude of NPQ induction was substantially smaller in the *npq4* mutant compared to WT during light treatment, and further reduced in *npq4 lhcsr1* (Fig. 3A–C). In addition, the NPQ kinetics of the latter genotype differed from WT and *npq4* by a far slower recovery from the quenched state in the dark, suggesting

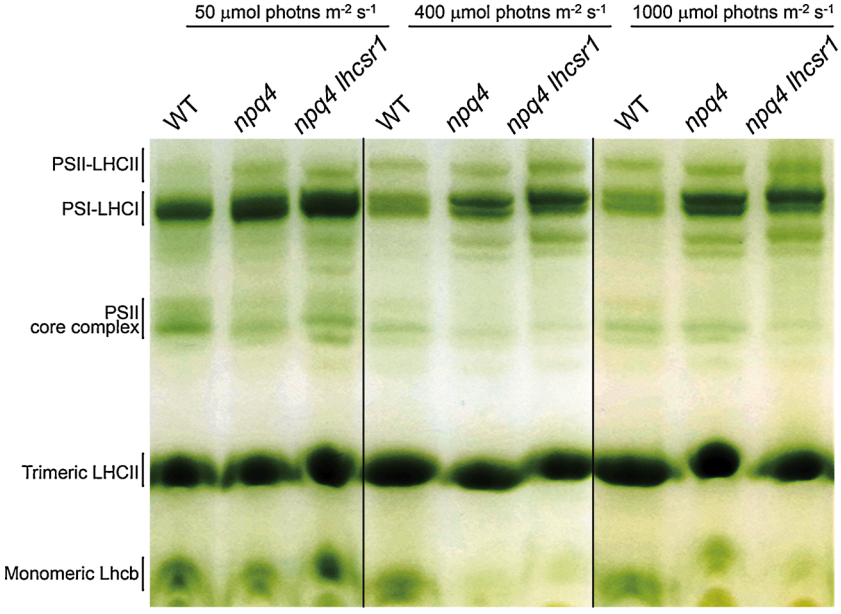

Fig. 2. Organization of thylakoid pigment-protein complexes. Thylakoids were isolated from cells growth under different continuous light regimes (indicates on the top). Chlorophyll-binding complexes were separated by nondenaturing Deriphat-PAGE upon solubilization of thylakoids with 2% α-DM. Membranes corresponding to 20 µg of chlorophylls were loaded in each lane. Composition of the major protein bands are indicated. (For interpretation of the references to colour in this figure legend, the reader is referred to the web version of this article.)

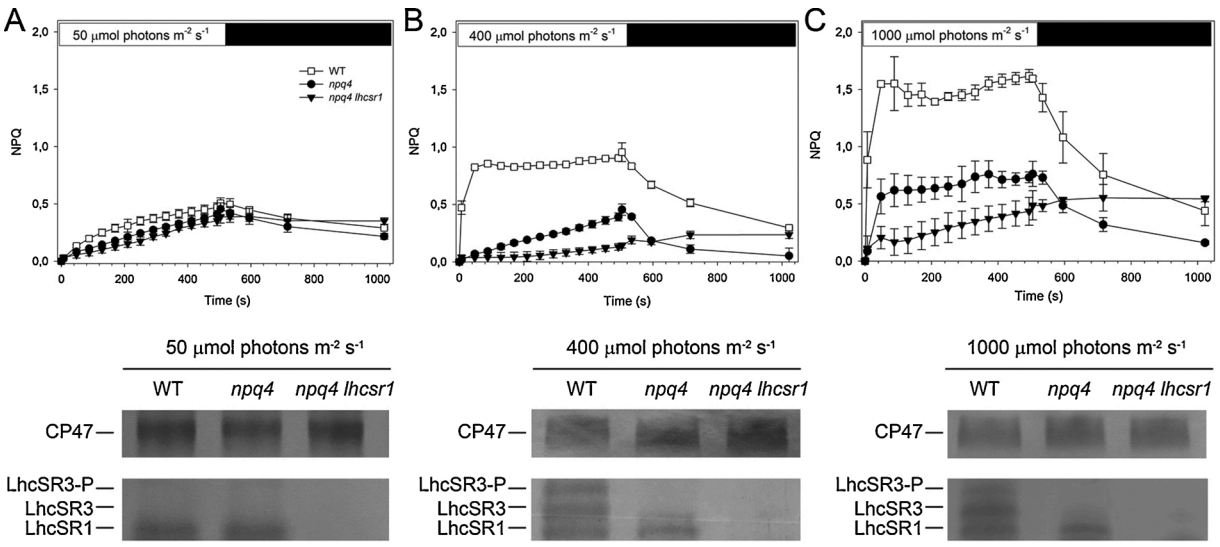

Fig. 3. Kinetics of non-photochemical quenching (NPQ) rise and decay. (A-C, upper panels) NPQ induction and relaxation kinetics were measured on WT, *npq4* and *npq4 lhcsr1* strains, acclimated for (8, 5 and 5) days respectively to different light regimes: 50 (panel A), 400 (panel B) or 1000 μmol photons m^{-2} s^{-1} (panel C)., NPQ was induced by illuminating dark-adapted cells with actinic light (1600 μmol photons m^{-2} s^{-1}) for 8 min followed by dark recovery. A far-red light (10 μmol photons m^{-2} s^{-1}) was used in order to maintain state I conditions during recovery. Data are expressed as mean ± SD, n = 3 biologically independent samples. Statistical analysis (ANOVA followed by Tukey's post test at a significant level of $P < 0.05$) revealed significantly different NPQ amplitudes among genotypes under illumination (WT > *npq4* > *npq4 lhcsr*1), with the exception of *npq* genotypes at 50 μmol photons m^{-2} s^{-1} ($P > 0.07$). (A-C, lower panels) Immunoblotting was used for the quantification of LhcSR subunits in protein extracts from WT and *npq* cells used for NPQ measurements. Analysis was performed with specific α-LHCSR and α-CP47 antibody. Total proteins corresponding to 1 μg of Chls were loaded for each sample, all samples were loaded on the same SDS-PAGE slab gel. The α-LHCSR antibody recognizes three LhcsR protein isoforms: LHCSR3-P (phosphorylated form), LHCSR3 and LHCSR1. (For interpretation of the references to colour in this figure legend, the reader is referred to the web version of this article.)

photo-inhibition occurred during the 8 min of excess of light (EL) exposure.

Singlet Oxygen Release. NPQ activity is thought to prevent over-excitation and production of $^1O_2$ from charge recombination in PSII. In order to verify whether the level of NPQ activity was correlated to $^1O_2$ release *in vivo*, we incubated cells at 850 μmol photons m^{-2} s^{-1}, 25 °C in the presence of SOSG, a $^1O_2$-specific fluorescent probe (Flors et al., 2006a) SOSG fluorescence was measured over a period of 6 h (Fig. 4). During the first hour all samples yielded the same emission at 532 nm, after which they differentiated into *npq4 lhcsr1* > *npq4* > WT. Interestingly, $^1O_2$ release in WT levelled at times > 150 min while a further increase was observed in both *npq4* and *npq4 lhcsr1*. In the latter genotype, the best fitting for the dataset was linear for cell grown at 50 μmol photons m^{-2} s^{-1} (Fig. 4A), implying that in the absence of NPQ activity $^1O_2$ release was proportional to irradiation. Instead, in *npq4* and WT with residual or full quenching activity, the $^1O_2$ release was substantially lower *i.e.* to 40% in WT and 55% in *npq4* in respect for *npq4 lhcsr*, and showed a decrease of probe emission rate after 3 h of irradiation, particularly with cells grown at HL (Fig. 4C).

Photoinhibition. NPQ mutant strains and the respective wild type grown at different light regimes (50, 400 and 1000 μmol photons m^{-2} s^{-1}, 25 °C) were exposed to EL, 1600 μmol photons m^{-2} s^{-1}, at 25 °C for 3 h in order to compare the rate of photoinhibition occurring in each strain (Fig. 5A–C). Fv/Fm values measured at time zero (just before EL treatment) and at the end of the recovery are reported in Fig. 5D, showing quantum yield of PSII was similar in the three strains when grown in LL, while clearly differentiate in the *npq* mutant strains grown at 400 μmol photons m^{-2} s^{-1} or above, with a stronger decrease in *npq4 lhcsr1 versus. npq4*. The EL treatment caused stronger decline in Fv/Fm in *npq4* and *npq4 lhcsr1* in respect for the WT for each light growth condition, while the recovery in dim light showed a similar kinetics, irrespective from the genotype. Instead the recovery rate was lower in

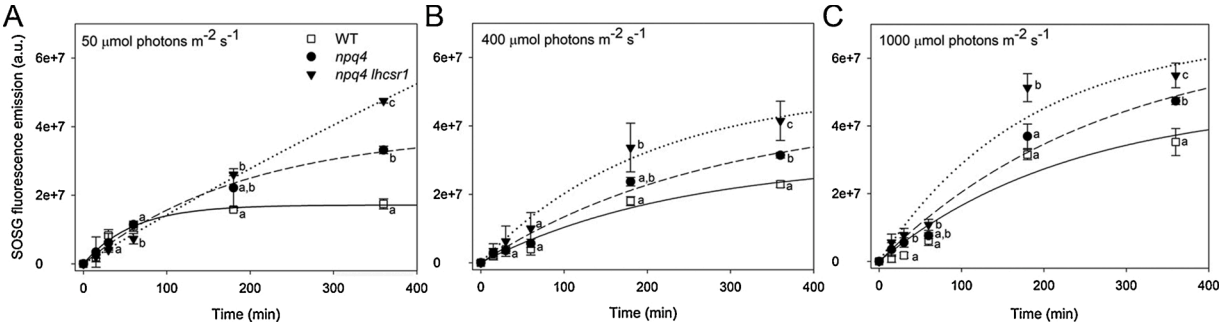

Fig. 4. *In vivo* singlet oxygen release in WT, *npq4* and *npq4 lhcsr1* strains. Cell suspensions form WT and mutant strains, acclimated for (8, 5 and 5) days respectively to different light regimes (50 μmol photons m^{-2} s^{-1}, panel A; 400 μmol photons m^{-2} s^{-1}, panel B; 1000 μmol photons m^{-2} s^{-1}, panel C) were treated with SOSG, a $^1O_2$-specific fluorogenic probe, which increases its fluorescence emission upon reaction with the ROS. The increase in the probe emission was followed upon illumination with red actinic light (550 μmol photons m^{-2} s^{-1}) at 25 °C. a.u., arbitrary units. Data are shown as mean ± SD, n = 3 biologically independent samples. Values marked with different letters are significantly different from each other at the same light intensity (ANOVA followed by Tukey's post test at a significant level of $P < 0.05$). (For interpretation of the references to colour in this figure legend, the reader is referred to the web version of this article.)

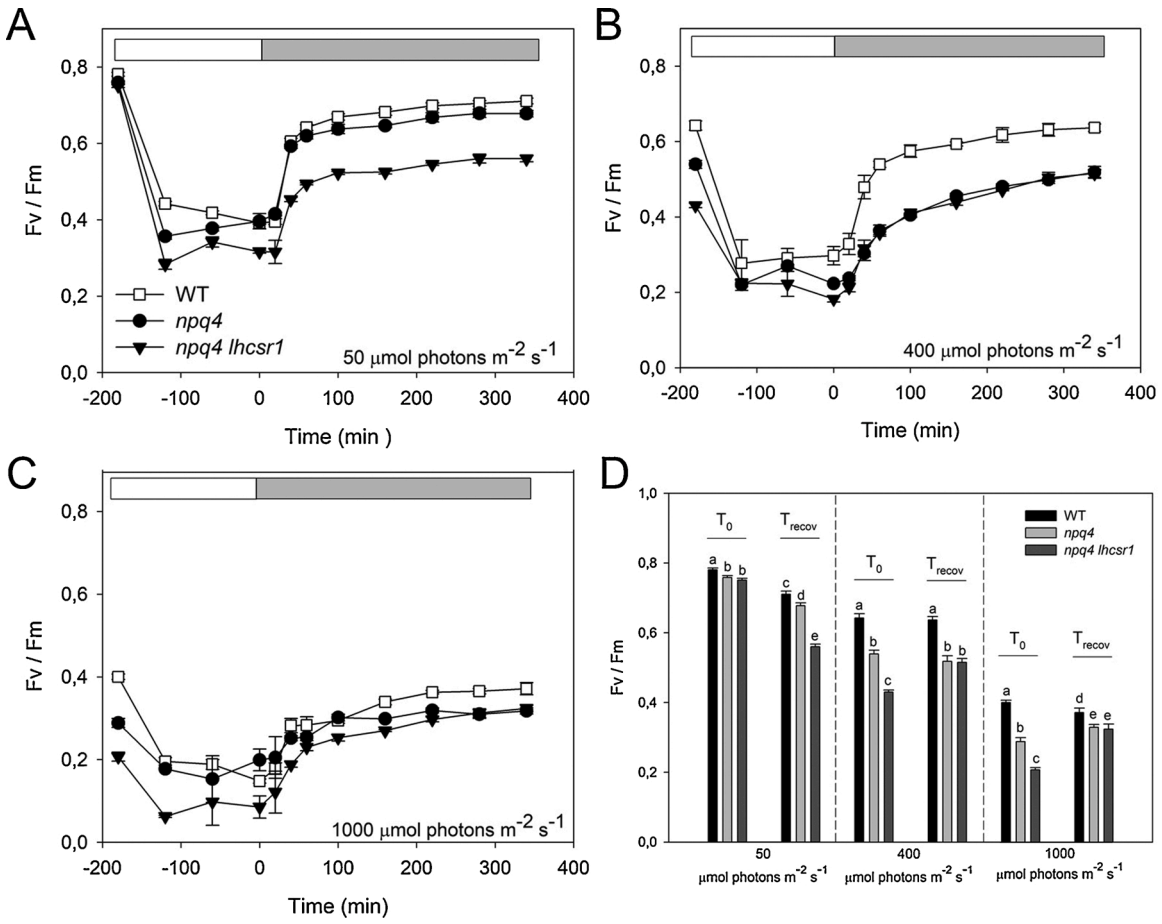

Fig. 5. PSII photoinhibition and repair efficiency under EL conditions. (A-C) PSII repair efficiency was quantified on WT, *npq4* and *npq4 lhcsr1* strains grown in different light conditions (50, 400 and 1000 µmol photons m^{-2} s^{-1} respectively in panel A, B and C). Fv/Fm (PSII photoinhibition) was measured during 3-h EL (1800 µmol photons m^{-2} s^{-1}, 24 °C) treatment and recovery at 20 µmol photons m^{-2} s^{-1}, 24 °C. (D) For each growth conditions, Fv/Fm values measured at time zero (T_0) and at the end of the LL recovery (T_{RECOV}) are displayed. Data are expressed as mean ± SD (n = 3) biologically independent samples. Values marked with different letters are significantly different from each other at the same growth irradiance (ANOVA followed by Tukey's post test at a significant level of $P < 0.05$).

HL acclimated cells and never the Fv/Fm values exceeded those measured previous to EL treatment (Fig. 5C), suggesting that growth in HL had set an acclimatative status of low PSII quantum yield.

2.4. Growth curves and productivity at different light regimes

The productivity of *WT, npq4* and *npq4 lhcsr1* cells was investigated by following growth in batch airlift PBRs, at 25 °C and different irradiances, either continuous or intermittent, provided by white light LEDs. Intermittent light growth was measured with either rapid (1 s) or slower (5 min) switching from light to dark, at either 400 or 800 µmol photons m^{-2} s^{-1} (Table 2).

Table 2
Light regimes, photoperiod and feeding gas used for growing WT and mutant strains in each experiment. Each experiment was performed in at least four biological replicates in independent PBRs. Light intensity and photoperiod used are reported. See material and methods for details.

Experiment	Light Intensity (µmol photons m^{-2} s^{-1})	Photoperiod	Feeding gas
A	20	Continuous	Air
B	50	Continuous	Air
C	200	Continuous	Air
D	400	Continuous	Air
E	800	Continuous	Air
F	1000	Continuous	Air
G	400	1 s light / 1 s dark	Air
H	800	1 s light / 1 s dark	Air
I	400	5 min light / 5 min dark	Air
J	800	5 min light / 5 min dark	Air
K	200	Continuous	Air + CO_2

Growth rate under continuous light was measured at 20, 50, 200, 400, 800 and 1000 µmol photons m^{-2} s^{-1} (Fig. 6, panels A to F, respectively) and intermittent light at 400 and 800 µmol photons m^{-2} s^{-1}, either 1 s of light followed by 1 s dark, or 5 min light followed by 5 min dark (Fig. 7, panels A–B and C–D respectively), by continuous measurements of optical density (OD). At both 20 and 50 µmol photons m^{-2} s^{-1} growth of WT appeared slightly slower in respect for *npq4* and *npq4 lhcsr1* and yet within the error of the measurements (Fig. 6A–B, G). At higher light intensity, *i.e.* 200 and 400 µmol photons m^{-2} s^{-1}, no significant differences in growth could be detected (Fig. 6C–D, G); at 200 µmol photons m^{-2} s^{-1} growth of WT and *npq4 lhcsr1* was slightly lower than *npq4* between 1 and 3 days, however it recovered to the same level at later times. At 800 µmol photons m^{-2} s^{-1}, *npq4* and *npq4 lhcsr1* showed an earlier reach of saturation level at t > 3 days, while no significant differences were obtained when comparing WT with the different mutants at 1000 µmol photons m^{-2} s^{-1} (Fig. 6E-F, G). At intermittent 400 µmol photons m^{-2} s^{-1}, 1 s light / 1 s dark (Fig. 7A, E), no differences could be detected among genotypes within the error of the measurement; while, under 1 s intermittent 800 µmol photons m^{-2} s^{-1} (Fig. 7B, E) *npq4 lhcsr1* growth faster than *npq4* while WT performed in between. Interestingly, intermittent light 5 min light / 5 min dark, for

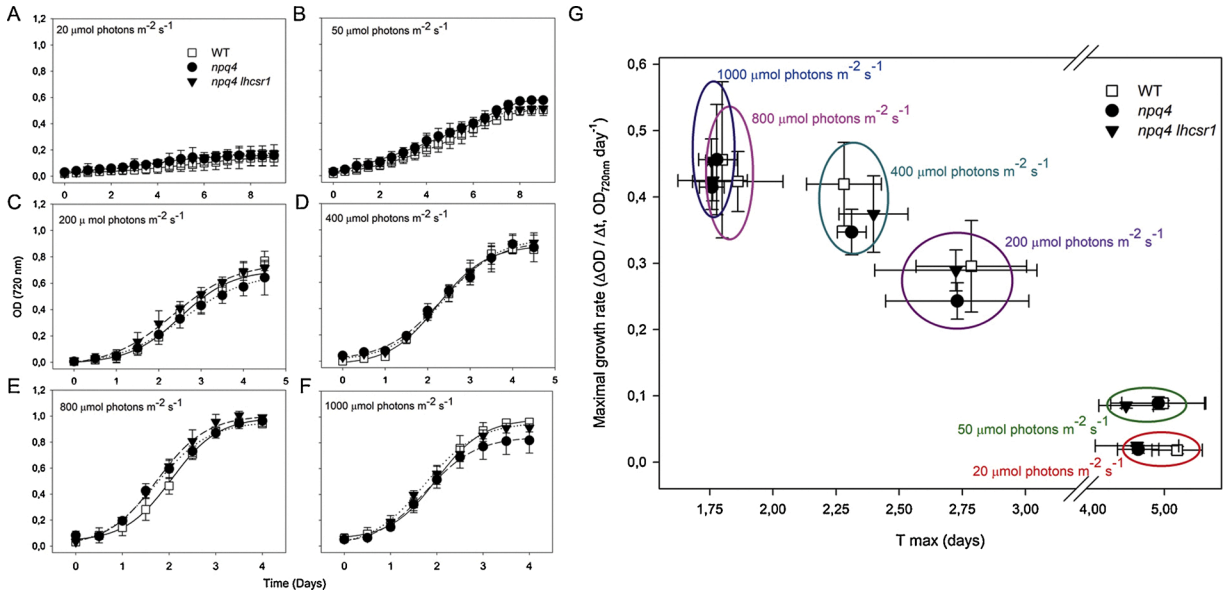

Fig. 6. Growth curves of WT and mutant strains under different continuous light regimes. (A—F) Time-dependent course of cell proliferation. Each experiment was performed in 8 tubes of a lab-scale PBR, growth was monitored by following the OD values at 720 nm. Irradiances used are indicated in each panel. Data are expressed as mean ± SD, n = 4. Experimental points were fitted with sigmoidal functions. (G) Maxima values of the first derivate of the sigmoidal curves (∂OD/∂t) *versus.* time of the maximal growth were plotted to pinpoint the maximum productivity and when it was reached. Group of data measured at the different light regimes in WT (square), *npq4* (circle) and *npq4 lhscr1* (triangle) are hooped with different colours.

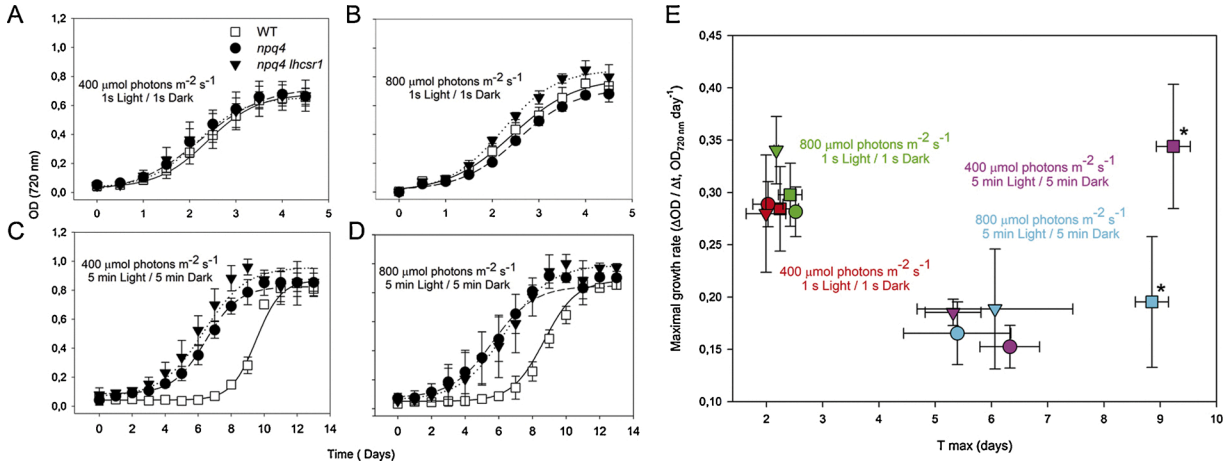

Fig. 7. Growth curves of WT and mutant strains under different fluctuating light regimes. (A-D) Time-dependent course of cell proliferation. Each experiment was performed in the same PBR of Fig. 6. Irradiances and photoperiods used are indicated in each panel. Data are expressed as mean ± SD, n = 4. Experimental points were fitted with sigmoidal functions. (E) Maxima values of the first derivate of the sigmoidal curves (∂OD/∂t) *versus.* time of the maximal growth were plotted to pinpoint the maximum productivity and when it was reached. Data measured at the different light regimes in WT (square), *npq4* (circle) and *npq4 lhscr1* (triangle) are marked with different colours. WT strain grown under 5 min fluctuating light regime showed significantly slower growth (indicated by asterisks) than *npq* lines (two-sided Student's *t*-test, $P < 0.05$).

both light irradiances *npq* mutants showed a significantly faster growth kinetics and a shorter lag phase in respect for the WT (Fig. 7C–E). The derivative analysis of the growth kinetics (Figs. 6G) showed that the fastest growth phase was observed around day 4.5–5 at 20 and 50 µmol photons m^{-2} s^{-1}, around day 2.2–2.7 at 200 and 400 µmol photons m^{-2} s^{-1} and day 1.7–1.9 at higher irradiances, with no differences between genotypes but with max growth rate increasing with light intensity up to 800 µmol photons m^{-2} s^{-1} (Fig. 6G). Under 1 s intermittent light and continuous light with the same average photon flux the growth was similar (Fig. 7E), and no difference was observed between genotypes at 400 µmol photons m^{-2} s^{-1}. At 800 µmol photons m^{-2} s^{-1}, small differences were observed with *npq4 lhcsr1* growing slightly faster than both WT and *npq4*, somehow slower. Yet, the differences were very small, if any, within the error of the measurements. Under slow switching light/dark regimes clear difference was observed in WT strain, undergoing a longer lag phase, with in respect for *npq4* and *npq4 lhcsr1*. Although delayed, maximum growth rate was higher in WT in respect for *npq4* and *npq4 lhcsr1* genotypes at 400 µmol photons m^{-2} s^{-1}, and intermediate at 800 µmol photons m^{-2} s^{-1} (Fig. 7E).

Analysis of pigment content of cells grown under fast and slow switching intermittent light showed the Chl *a/b* ratios was maintained roughly the same than control condition (50 µmol photons m^{-2} s^{-1} continuous light) in all genotypes (Table 1). Instead, Chl content per cell was reduced to the same extent in all genotypes at increasing irradiances; the functional antenna size of PSII, quantified on cell suspensions by estimating the rise time of Chl *a* fluorescence, was essentially the

same at 400 µmol photons m^{-2} s^{-1} than control conditions, while strongly reduced at 800 µmol photons m^{-2} s^{-1} to the same extent (-30%) in all genotypes (Table 1). Because Chl *b* is a component of light-harvesting antenna systems of both PSI and PSII, but is more abundant in the latter, this result suggests that acclimation to 800 µmol photons m^{-2} s^{-1} / 5 min fluctuating light conditions does influence not only PSII antenna sizes in *C. reinhardtii*, but also PSI/PSII ratio.

When algae reached the stationary phase, analysis of pigments content and immuno-titration with α-LHCSR antibody were carried out for each growth experiments (see Figure S1). Upon the cultures reached saturation, the biomass was harvested and the dry weight (DW) measured (Fig. 8A). The productivity under continuous light regimes ranged from 0.11 to 0.75 g L^{-1}. Under intermittent light of 400 µmol photons m^{-2} s^{-1} biomass recovered was ~0.45 g L^{-1}, very similar to that obtained with 200 µmol photons m^{-2} s^{-1} continuous light, *i.e.* with the same integrated photon supply. Biomass recovered under fast intermittent light was slightly lower at 800 µmol photons m^{-2} s^{-1} (Fig. 8A) than at 400 µmol photons m^{-2} s^{-1}, and lower than at 400 µmol photons m^{-2} s^{-1} continuous light, implying that light saturation effect was exacerbated under rapidly intermittent light in respect for the case of continuous light. Under 5 min intermittent light at 400 µmol photons m^{-2} s^{-1}, biomass accumulated was slightly lower than under continuous light with the same photon flux. Doubling light intensity to 800 µmol photons m^{-2} s^{-1}, however released the saturation effect thus reaching the same biomass as obtained with 1000 µmol photons m^{-2} s^{-1} of continuous light (Fig. 8A).

The conversion efficiency of light into stored chemical energy was estimated by calculating the photon conversion efficiency (PCE) (Bonente et al., 2012) as the ratio between the DW recovered and the average light intensity available during growth (Fig. 8B). In agreement with previous results (Bonente et al., 2012), PCE decreased with increasing growth light intensities ($20 > 50 > 200 > 400 > 800 = 1000$ µmol photons m^{-2} s^{-1} continuous light) for all the strains analysed. Under fast pulsed light regimes, the PCE was similar for the three genotypes but for the case of *npq4 lhcsr1* grown at 800 µmol photons m^{-2} s^{-1} which was slightly higher than WT and *npq4*. Under 5 min intermittent light regime at 800 µ mol photons m^{-2} s^{-1}, PCE was decreased by 40% in respect for the culture grown at 400 µ mol photons m^{-2} s^{-1} fast switching intermittent light, and only slightly lower than under continuous light of the same average photon flux. Growth under 5 min intermittent light had the strongest effect on PCE, halving the efficiency of energy conversion in respect for the condition of the same photon flux delivered in continuous light or with 1 s pulse. Doubling photon supply further decreased PCE reaching the level of cultures grown under continuous 1000 µmol photons m^{-2} s^{-1}, which was the lowest determined in this study.

Decreasing heat dissipation is expected to enhance the excitation pressure and, possibly, the availability of reducing equivalents for CO_2 reduction and/or reactive oxygen species formation. The availability of CO_2 substrate for RuBisCO is thus a limiting factor for biomass accumulation and might well affect the growth phenotype of the strains analysed in this study. In order to assess whether the availability of high CO_2 was a pre-requisite for enhancement of productivity caused by the mutation, we proceeded to a comparative growth analysis with and without added CO_2 in a home-built, semi-batch PBRs under near-saturating light intensity (200 µmol photons m^{-2} s^{-1}, 25 °C). Results in Figure S2 show that CO_2 supplementation induced a limited enhancement in DW accumulation of about 7–8% in respect for non-supplemented cultures (Figure S2A). However, the lag-phase in growth kinetics (Figure S2B) and the PCE values (Figure S2C) were similar irrespective from CO_2 supplementation or not, and the growth rate was very similar for all strains and conditions.

3. Discussion

Energy dissipation limits growth and enhances photoprotection thus avoiding photoinhibition. Photoinhibition is caused by reactive oxygen species originated by charge recombination in PSII, yielding mainly $^1O_2$. Photosynthetic organisms exposed to high irradiance have evolved the ability to switch to quenching states to safely dissipate the energy absorbed in excess into heat. Under limiting light conditions, it was shown that *Arabidopsis* genotypes either lacking or constitutively enhanced in energy dissipation respectively enhanced or decreased their biomass accumulation rate thus establishing *in vivo* an inverse relation between energy dissipation and growth (Dall'Osto et al., 2005). More recently, engineering of tobacco plants for faster NPQ relaxation, thus decreasing the integrated heat dissipation, yielded into significant enhancement of biomass production in field conditions (Kromdijk et al., 2016). Attempts to implement this strategy in algae yielded contrasting results: the growth rate in PBR of the *Chlamydomonas npq4* mutant was reported to be higher in respect for WT (Perozeni et al., 2018) or not (Chaux et al., 2017) (Cantrell e Peers, 2017). These evidences leave open the question of whether down-regulation of NPQ can be an useful strategy for increasing light use efficiency in biomass production. In unicellular algae, energy dissipation is catalysed through protonation of the pigment-binding LHCSR proteins (Bonente et al., 2011) conversely, in higher plants qE is triggered by protonation of the pigment-less PSBS

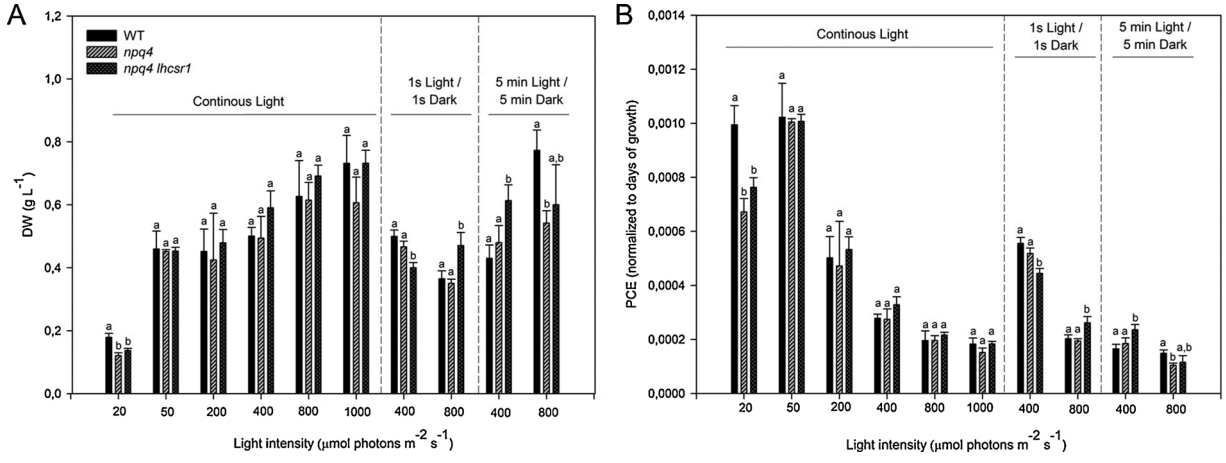

Fig. 8. Biomass production and photon conversion efficiency of WT, *npq4* and *npq4 lhcsr1* strains. (A) Biomass produced as g DW L^{-1} of WT and *npq* strains, grown at the different light regimes indicated in the figure. (B) Photon conversion efficiency (PCE) was calculated as the ratio between the DW of biomass and the average photon flux density [(g L^{-1})/(µmol photons m^{-2} s^{-1})], normalized to the days of growth (see Figs. 6,7). Data are expressed as mean ± SD, n = 3 biologically independent samples. Values marked with different letters are significantly different from each other at the same growth irradiance (ANOVA followed by Tukey's post test at a significant level of $P < 0.05$).

protein (Li et al., 2002), (Dominici et al., 2002), (Fan et al., 2015). PSBS and LHCSR are localized in different thylakoid membrane domains: PSBS in grana membranes together with PSII (Redekop et al., 2020) (Pinnola et al., 2015b), (Dikaios et al., 2019) while LHCSR is in stroma membranes where it can act on both PSI and PSII (Pinnola et al., 2015a), (Girolomoni et al., 2019).

3.1. NPQ and protection from photoinhibition

The presence of LHCSR clearly influenced the resistance to photoinhibition of *Chlamydomonas* cells, as shown from the differential effect of acclimation at different light intensities: at LL, Fv/Fm was high and equal on the three genotypes; however, with increasing light intensity PSII quantum yield decreased faster in *npq4* and even more in *npq4 lhcsr1* in respect for WT (Fig. 5). WT cells growth in high light showed PSII quantum yield of ~50% in respect for LL treatment while *npq4* and *npq4lhcsr1* showed Fv/Fm values respectively 37 and 25% of WT growth in LL. Fv/Fm further decreased during 3 h strong light treatment in all genotypes and upon acclimation in all light conditions. However, the decrease in Fv/Fm was stronger in LL acclimated cells in respect for those acclimated at HL (Fig. 5). Also, both ML and HL *npq4* and *npq4lhcsr1* were slightly less affected by the treatment in respect for WT, suggesting that acclimation to increasing photon flux enhanced the resistance to further light stress by LHCSR-independent(s) mechanism (s). It is interesting to note that recovery under dim light showed a similar half-time in all genotypes (Fig. 5A–C) implying that the repair capacity was not modulated by acclimation to light conditions and was independent from the presence of LHCSR, while its location in stroma membranes together with PSII repair cycle (Mattoo et al., 1989) might have suggested a positive correlation. Also, repair in dim light for up to 6 h led to saturation of Fv/Fm recovery at values similar to those observed previous to the photoinhibitory treatment rather than those typical of LL grown cells (Fig. 5A), suggesting that acclimation in EL induced long-term resistance mechanisms which, while decreasing Fv/Fm, where independent from PSII damage/repair cycle. The observation that $^1O_2$ release was higher in WT *versus*. *npq4* and *npq4 lhcsr1* and further, was enhanced with increasing light, is consistent with such repair mechanisms being $^1O_2$-activated through signalling by β-carotene catabolites, as proposed by (D'Alessandro and Havaux, 2019). Immunological analysis of protein markers for PSII, LHCII, PSI, Cyt b_6f, ATPase and Calvin cycle (RuBisCO) showed that stoichiometry between the major component of the photosynthetic apparatus was maintained within 10% with the exception of a 30% increase in PSI of *npq4 lhcsr1* (Figs. 1B–C, 2). While *npq4* and *npq4 lhcsr1* showed a continuous increase in $^1O_2$ release depending on light intensity, WT only did that at 1000 μmol photons m^{-2} s^{-1}, implying that NPQ activity by LHCSR did contain $^1O_2$ production till 400 μmol photons m^{-2} s^{-1} at least, but not at 1000 μmol photons m^{-2} s^{-1} (Fig. 4A–C).

3.2. Effects of NPQ modulation on biomass productivity

Initial characterization of WT, *npq4* and *npq4 lhcsr1* strains showed higher O_2 evolution in the LHCSR-less mutant, in HL conditions (irradiance > 500 μmol photons m^{-2} s^{-1}) (Fig. 1A), suggesting that decreasing excess energy dissipation might indeed increase productivity. However, the observation that *npq4*, although showing a strongly decreased NPQ activity, did not show O_2 evolution rate similar to WT was inconsistent with this hypothesis. Also, enhanced growth of *Arabidopsis npq4* (Dall'Osto et al., 2005) was previously observed in light limiting conditions where enhanced excitation energy might arguably be effective in shifting electron transport towards saturation rather than in very EL, a condition in which enhancing excitation pressure on PSII should not enhance CO_2 fixation by an already saturated Calvin-Benson cycle. We hypothesize that enhanced O_2 production by *npq4 lhcsr1* in HL derives from the enhanced PSI/PSII ratio in this strain (Figs. 1,2). This might contribute to decrease over-reduction of PQ pool in HL conditions. More PSI could lead to enhanced cyclic electron transfer *via* PGRL1/Pgr5; nevertheless, an enhanced APP production should correspond to higher levels of ATPase, which we did not observe (Fig. 1). Thus we favour the alternative hypothesis that excess reducing power is dissipated through PTOX or Flavodiiron protein activity. We did not further analyse the fate of reducing equivalent in these genotypes because it was outside the major aim of this work. We notice that the enhanced PSI in *npq4 lhcsr1* correlated with a strongly enhanced $^1O_2$ release in this mutant (Fig. 4), likely inducing an enhanced state of acclimation (D'Alessandro and Havaux, 2019), to an higher extent in respect for WT and *npq4*, which might involve additional electron sinks whose identity will be the subject of forthcoming studies.

In this work, we assessed productivity of the three genotypes in a wide range of light conditions, from 20 to 1000 μmol photons m^{-2} s^{-1} of continuous light. In each of the 6 light intensities, growth kinetics were very similar between the genotypes within experimental errors. There were small differences, but these were not consistent across conditions: *e.g. npq4* was performed slightly better in respect for WT under light B, but slightly worse under light C and F (Fig. 6, Table 2). The final biomass produced in these growth experiments was also very similar across genotypes with *npq4*, if any, performing slightly worse in respect for both WT and *npq4 lhcsr1* (Fig. 8A). The PCE (photon conversion efficiency) in building biomass (Fig. 8B) was maximal at 50 μmol photons m^{-2} s^{-1}, with all genotypes performing the same. WT performed significantly better in respect for *npq4* and *npq4 lhcsr1* in very dim light only. These results are in contrast with previous reports (Berteotti et al., 2016) which showed strongly enhanced PCE in *npq4* in respect for both WT and *npq4 lhcsr1*, particularly at near-saturating light intensity.

In PBRs, algae undergo rapid changes in light intensity due to mixing of the liquid medium and shading by other cells. We assessed growth curves and productivity under two intermittent light regimes with either fast (1 s) or slow (5 min) switching from light to dark, and two averaged photon fluencies. Under rapidly fluctuating light, algae performed similar, although slightly lower, to continuous light with same averaged photon fluency. Under slowly fluctuating irradiance, with light periods allowing for full expression of NPQ (Fig. 3) the differences between genotypes were more evident with WT being delayed in growth by 3–4 days in respect for *npq4* and *npq4 lhcsr1*. It should be noticed, however, that once growth was resumed, the rate was as fast in WT as in *npq4* and *npq4 lhcsr1* (Fig. 7). We conclude that, rapidly intermittent light did not differentiate between genotypes while the growth of NPQ-competent WT was impaired under relatively long photoperiod. Again, all genotypes performed similarly in light use efficiency, but for a delay in the onset of growth in WT (Fig. 8B).

Our last question was of whether the availability of CO_2, the final electron acceptor for photosynthetic electron transport, might limit productivity and therefore mask the differential effect of energy dissipation in different genotypes. The results of Figure S2, in which growth with and without CO_2 supplementation is compared, clearly exclude this possibility since all genotypes performed the same, irrespective from NPQ activity and CO_2 supplementation at half saturating light condition (200 μmol photons m^{-2} s^{-1}).

We conclude that within the limits of our range of experimental conditions, which is, however, far wider in respect for that of previous studies (Berteotti et al., 2016) (Chaux et al., 2017), no enhancement of productivity was evidenced growth of genotypes with decreased NPQ activity. Thus, down-regulating NPQ as a strategy towards enhancement of algal productivity is ineffective according to our results.

Since the present study was performed by using the same strains and the same PBRs as in a previous report (Berteotti et al., 2016), we retracted the earlier report (Berteotti et al., 2016) which contained results that could not be confirmed in many independent measurements reported here.

4. Experimental procedures

4.1. Cell cultivation

Chlamydomonas reinhardtii wild type strain (WT137 mt+) and mutants *npq4* and *npq4 lhcsr1* (kindly gifted by Niyogi K.K. and described in (Peers et al., 2009b) and (Ballottari et al., 2016) were analysed in this work. Additional *npq4* mutant lines (CC-4614 and CC-4615) were obtained from Chlamydomonas Resource Center, University of Minnesota; these lines were obtained from the original *npq4* mutant (Niyogi et al., 1997) upon backcrossing four times to the 4a + strain (Truong, 2011) *npq4*, CC-4614 and CC-4615 lines showed very similar growth kinetics and photon use efficiency (Figure S3). The original *npq4* line (Niyogi et al., 1997) was used in the present work for both the functional characterization and the growth curves. Cells were grown photoautotrophically in HS medium (Sueoka, 1960), in either flasks (50 µmol photons m^{-2} s^{-1} white light provided by warm-white fluorescence lamps, 25 °C, photoperiod of 16/8 h light/dark, orbital shacking at 150 rpm) or laboratory-scale PBR (Multi-Cultivator MC 1000, Photon System Instruments, Brno, Czech Republic) at 25 °C. In the latter, each of the 8 test-tubes, bubbled with air, was controlled in real time for both the turbidity and the absorption of chlorophyll. For physiological measurements, cultures were harvested during the logarithmic growth phase (~1−3·10^7 cells ml^{-1}). Each experiment started with 3·10^5 cells ml^{-1} in HS medium enriched with CO_2 sources ($NaHCO_3$ 0.5 g/L, Applichem GmbH, Darmstadt, Germany, cat. Number 131,638). The cultures were grown for one day under 50µ mol photons m^{-2} s^{-1}, and after that, the different light intensity/photoperiod regimes (Table 2) were applied. Medium-scale growth experiments were performed in HS medium at 25 °C, in a home-built laboratory-scale PBR, semi-batch cultivation system composed of 1-L glass cylinders, with a maximum light path of 8 cm, illuminated by warm-white LED (200 µmol photons m^{-2} s^{-1}). The system was fed with a flux of air and CO_2, whose relative abundance was regulated by the pH of the medium in order to keep within the range of 6.8 to 7.1. Each autotrophic batch cultivation was carried out in duplicate. The parameters determined to monitor cell growth were cell number and DW, for which the washed cell pellets were dried overnight in a lyophilizer.

4.2. Growth analysis

Growth in the PBR MC 1000 tubes was automatically monitored every 12 h by measuring cell dependent scattering at 720 nm. The initial inoculum was 3·10^5 cells ml^{-1}, corresponding to an OD of 0.007 ± 0.003 at 720 nm. Cell density was measured using an improved Neubauer hemocytometer Biomass DW was estimated upon washing cell pellets and drying biomass overnight in a lyophilizer.

4.3. Pigment analysis

Pigments were extracted from intact cells with 85% acetone (Honeywell Riedel-de Haen™, cat. Number 31,062). The supernatant of each sample was recovered after centrifugation (10 min, 15,000*g*) and analysed. Pigment quantifications, chlorophyll to carotenoid ratio and Chl *a/b* ratio were independently measured by fitting the spectrum of acetone extracts with the spectra of individual purified pigments (Croce et al., 2002)

4.4. In vivo Chl fluorescence analysis

NPQ of chlorophyll fluorescence was measured on cell suspensions at room temperature (RT, 25 °C) with a PAM 101 fluorometer (Walz, Effeltrich, Germany) according to the equation defined by (Van Kooten e Snel, 1990) using a saturating light pulse of 3000 µmol photons m^{-2} s^{-1}, 0.6 s, and white actinic light of 1600 µmol photons m^{-2} s^{-1}. Before measurements, cells were dark-adapted under stirring for at least 60 min.

4.5. Measurements of photosynthetic activity

The O_2 evolution activity of the cultures was measured at RT with a Clark-type O_2 electrode (Hansatech, UK) upon illumination with white light provided by a halogen lamp (Schott, Germany). Samples of 2 mL cell suspension (~ 5·10^7 cell ml^{-1}, in HS medium) were loaded into the oxygen electrode chamber; 3 mM $NaHCO_3$ was added to the cell suspension prior to the O_2 evolution measurements to ensure electron transport was not limited by the carbon supply.

4.6. Determination of the sensitivity to photoxidative stress

EL treatment was performed for 3 h at 1800 µmol photons m^{-2} s^{-1} white light, followed by 6 h of recovery at 20 µmol photons m^{-2} s^{-1}, at RT. Quantitative evaluation was done by transferring 2 mL aliquots of WT and mutant cell suspensions (~5·10^7 cell ml^{-1}, in HS medium) into a 24-well culture plate, kept on a rotary shaker and illuminated. Kinetics of maximal quantum yield of PSII photochemistry (Fv/Fm) were measured through Chl fluorescence on cell suspensions at RT with a FluorCam 800 M F (Photon System Instruments, Brno, Czech Republic).

4.7. Isolation of thylakoid membranes

C. reinhardtii thylakoids were purified as previously described (Chua e Bennoun, 1975).

4.8. Gel electrophoresis and immunoblotting

For SDS-PAGE and immunotitration analysis, cells were resuspended in Loading Buffer (5% glycerol Honeywell, cat. number 49770, 1% SDS Applichem GmbH, Darmstadt, Germany, cat. number A4259, 2.5% 2-mercaptoethanol Applichem GmbH, Darmstadt, Germany, cat. number. A1108, 0.1 M Tris Applichem GmbH, Darmstadt, Germany, cat. number. A1086 pH 6.8). The supernatant of each sample was recovered after centrifugation (10 min at 15,000*g*). SDS-PAGE analysis was performed with the Laemmli (Laemmli, 1970) buffer system with the addition of 6 M urea in the resolving gel. Proteins were detected as described previously (Towbin et al., 1979) with primary antibodies (home-made: α-CP43, α-Rubisco, α-LhcSR; from Agrisera: α-PsaA AS06−172-100, α-Cyt*f* AS06−119, α-ATPase β subunit AS05−085) and an alkaline phosphatase-conjugated secondary antibody (Sigma-Aldrich A3687). Signal amplitude was quantified using the GelPro 3.2 software (Bio-Rad). Nondenaturing Deriphat-PAGE was performed as in (Peter e Thornber, 1991) but using 3.5% (w/v) acrylamide (38:1 acrylamide/bisacrylamide Applichem GmbH, Darmstadt, Germany, cat. number. A1577) in the stacking gel, and in the resolving gel an acrylamide concentration gradient from 4.5% to 11.5% (w/v) stabilized by a glycerol gradient from 8% to 16%. Thylakoids concentrated at 1 mg/mL Chl were solubilized with 1% α-DM (Anagrade, and 20 µg of Chls were loaded in each lane.

4.9. Masurement of $^1O_2$ release

Measurements of $^1O_2$ release were performed *in vivo* with a specific fluorogenic probe, singlet oxygen sensor green (SOSG, Invitrogen). SOSG is a $^1O_2$ highly selective fluorescent probe, that increases its 530-nm emission band in presence of this ROS species (Flors et al., 2006b). Cell suspensions (~ 5·10^7 cell ml^{-1}, in HS medium) were incubated with 100 µM SOSG, then illuminated with red light (λ > 600 nm) as previously described (Dall'Osto et al., 2010) Aliquots of cultures were harvested and SOSG fluorescence yield was measured using a Jobin-Yvon Fluoromax-3 spectrofluorometer.

4.10. Statistics

Significance analysis was performed using either Student's *t* test or

ANOVA test in GraphPad Prism software. Error bars represent the standard deviation.

Author contributions

S.B., L.D. and R.B. designed the experiments, S.B. performed the experiments, S.B., L.D. and R.B. analysed the data. R.B, L.D and S.B. wrote the manuscript. All authors have approved the final manuscript.

Data availability

All data are contained within the manuscript.

Funding and additional information

We acknowledge the financial support from the University-Industry Joint Projects “Hypercell” (grant JPVR 2016), Industrialgae (grant JPVR 2016) and the ENAC-2019 fund “Alternative fuels for civil aviation”.

Declaration of Competing Interest

The authors declare no conflict of interest.

Acknowledgments

We thank Prof. Krishna Niyogi (U.C. Berkeley) for the kind gift of Chlamydomonas *npq4* and *npq4lxhcsr1* strains and for discussions.

Appendix A. Supplementary data

Supplementary material related to this article can be found, in the online version, at doi:https://doi.org/10.1016/j.jbiotec.2020.12.023.

References

Ballottari, M., Truong, T.B., De Re, E., Erickson, E., Stella, G.R., Fleming, G.R., Bassi, R., Niyogi, K.K., 2016. Identification of pH-sensing sites in the light harvesting complex stress-related 3 protein essential for triggering non-photochemical quenching in *Chlamydomonas reinhardtii*. J. Biol. Chem. 291, 7334–7346. https://doi.org/10.1074/jbc.M115.704601.

Barber, J., 2009. Photosynthetic energy conversion: natural and artificial. Chem. Soc. Rev. 38, 185–196. https://doi.org/10.1039/b802262n.

Benedetti, M., Vecchi, V., Barera, S., Dall’Osto, L., 2018. Biomass from microalgae: the potential of domestication towards sustainable biofactories. Microb. Cell Fact. 17, 173. https://doi.org/10.1186/s12934-018-1019-3.

Berteotti, S., Ballottari, M., Bassi, R., 2016. Increased biomass productivity in green algae by tuning non-photochemical quenching. Sci. Rep. 6, 21339. https://doi.org/10.1038/srep21339.

Bonente, G., Ballottari, M., Truong, T.B., Morosinotto, T., Ahn, T.K., Fleming, G.R., Niyogi, K.K., Bassi, R., 2011. Analysis of LhcSR3, a protein essential for feedback de-excitation in the green alga *Chlamydomonas reinhardtii*. PLoS Biol. 9, e1000577.

Bonente, G., Pippa, S., Castellano, S., Bassi, R., Ballottari, M., 2012. Acclimation of Chlamydomonas reinhardtii to different growth irradiances. J. Biol. Chem. 287, 5833–5847. https://doi.org/10.1074/jbc.M111.304279.

Borowitzka, M.A., Moheimani, N.R., 2013. Algae for biofuels and energy. Algae for Biofuels and Energy. https://doi.org/10.1007/978-94-007-5479-9.

Cantrell, M., Peers, G., 2017. A mutant of Chlamydomonas without LHCSR maintains high rates of photosynthesis, but has reduced cell division rates in sinusoidal light conditions. PLoS One 12, e0179395. https://doi.org/10.1371/journal.pone.0179395.

Cazzaniga, S., Dall’Osto, L., Szaub, J., Scibilia, L., Ballottari, M., Purton, S., Bassi, R., 2014. Domestication of the green alga Chlorella sorokiniana: reduction of antenna size improves light-use efficiency in a photobioreactor. Biotechnol. Biofuels 7, 157. https://doi.org/10.1186/s13068-014-0157-z.

Chaux, F., Johnson, X., Auroy, P., Beyly-Adriano, A., Te, I., Cuiné, S., Peltier, G., 2017. PGRL1 and LHCSR3 compensate for each other in controlling photosynthesis and avoiding photosystem I photoinhibition during high light acclimation of Chlamydomonas cells. Mol. Plant. https://doi.org/10.1016/j.molp.2016.09.005.

Chua, N.H., Bennoun, P., 1975. Thylakoid membrane polypeptides of Chlamydomonas-reinhardtii - wild-type and mutant strains deficient in photosystem 2 reaction center. Proc. Natl. Acad. Sci. U. S. A. 72, 2175–2179.

Croce, R., Morosinotto, T., Castelletti, S., Breton, J., Bassi, R., 2002. The Lhca antenna complexes of higher plants photosystem I. Biochim. Biophys. Acta-Bioenergetics 1556, 29–40.

D’Alessandro, S., Havaux, M., 2019. Sensing β-carotene oxidation in photosystem II to master plant stress tolerance. New Phytol. https://doi.org/10.1111/nph.15924.

Dall’Osto, L., Caffarri, S., Bassi, R., 2005. A mechanism of nonphotochemical energy dissipation, independent from PsbS, revealed by a conformational change in the antenna protein CP26. Plant Cell 17, 1217–1232. https://doi.org/10.1105/tpc.104.030601.

Dall’Osto, L., Cazzaniga, S., Havaux, M., Bassi, R., 2010. Enhanced photoprotection by protein-bound vs free xanthophyll pools: a comparative analysis of chlorophyll *b* and xanthophyll biosynthesis mutants. Mol.Plant 3, 576–593.

Dall’Osto, L., Cazzaniga, S., Guardini, Z., Barera, S., Benedetti, M., Mannino, G., Maffei, M.E., Bassi, R., 2019. Combined resistance to oxidative stress and reduced antenna size enhance light-to-biomass conversion efficiency in Chlorella vulgaris cultures. Biotechnol. Biofuels 12, 221. https://doi.org/10.1186/s13068-019-1566-9.

Dikaios, I., Schiphorst, C., Dall’Osto, L., Alboresi, A., Bassi, R., Pinnola, A., 2019. Functional analysis of LHCSR1, a protein catalyzing NPQ in mosses, by heterologous expression in Arabidopsis thaliana. Photosynth. Res. https://doi.org/10.1007/s11120-019-00656-3.

Dominici, P., Caffarri, S., Armenante, F., Ceoldo, S., Crimi, M., Bassi, R., 2002. Biochemical properties of the PsbS subunit of photosystem II either purified from chloroplast or recombinant. J.Biol.Chem. 277, 22750–22758.

Fan, M., Li, M., Liu, Z., Cao, P., Pan, X., Zhang, H., Zhao, X., Zhang, J., Chang, W., 2015. Crystal structures of the PsbS protein essential for photoprotection in plants. Nat. Struct. &Amp; Mol. Biol. 22, 729.

Flors, C., Fryer, M.J., Waring, J., Reeder, B., Bechtold, U., Mullineaux, P.M., Nonell, S., Wilson, M.T., Baker, N.R., 2006a. Imaging the production of singlet oxygen in vivo using a new fluorescent sensor, Singlet Oxygen Sensor Green. J.Exp.Bot. 57, 1725–1734.

Flors, Cristina, Ogilby, P.R., Luis, J.G., Grillo, T.A., Izquierdo, L.R., Gentili, P.-L., Bussotti, L., Nonell, S., 2006b. Phototoxic phytoalexins. Processes that compete with the photosensitized production of singlet oxygen by 9-Phenylphenalenones†. Photochem. Photobiol. https://doi.org/10.1562/2005-04-07-ra-479.

Formighieri, C., Franck, F., Bassi, R., 2012. Regulation of the pigment optical density of an algal cell: filling the gap between photosynthetic productivity in the laboratory and in mass culture. J. Biotechnol. 162, 115–123. https://doi.org/10.1016/j.jbiotec.2012.02.021.

Girolomoni, L., Cazzaniga, S., Pinnola, A., Perozeni, F., Ballottari, M., Bassi, R., 2019. LHCSR3 is a nonphotochemical quencher of both photosystems in Chlamydomonas reinhardtii. Proc. Natl. Acad. Sci. U. S. A. https://doi.org/10.1073/pnas.1809812116.

Kromdijk, J., Głowacka, K., Leonelli, L., Gabilly, S.T., Iwai, M., Niyogi, K.K., Long, S.P., 2016. Improving photosynthesis and crop productivity by accelerating recovery from photoprotection. Science (80-.) 354, 857–861. https://doi.org/10.1126/science.aai8878.

Laemmli, U.K., 1970. Cleavage of structural proteins during the assembly of the head of bacteriophage T4. Nature. https://doi.org/10.1038/227680a0.

Li, X.P., Phippard, A., Pasari, J., Niyogi, K.K., 2002. Structure-function analysis of photosystem II subunit S (PsbS) in vivo. Funct. Plant Biol. 29, 1131–1139.

Li, Z., Wakao, S., Fischer, B.B., Niyogi, K.K., 2009. Sensing and responding to Excess Light Excess light (EL): a relative term that describes the absorption of light that exceeds photosynthetic capacity. Annu. Rev. Plant Biol. https://doi.org/10.1146/annurev.arplant.58.032806.103844.

Li, L., Aro, E.M., Millar, A.H., 2018. Mechanisms of Photodamage and Protein Turnover in Photoinhibition. Trends Plant Sci. https://doi.org/10.1016/j.tplants.2018.05.004.

Malkin, S., Armond, P.A., Mooney, H.A., Fork, D.C., 1981. Photosystem II photosynthetic unit sizes from fluorescence induction in leaves. Correlation to photosynthetic capacity. Plant Physiol. 67, 570–579.

Mattoo, A.K., Marder, J.B., Edelman, M., 1989. Dynamics of the photosystem II reaction center. Cell 56, 241–246.

Nelson, N., Ben-Shem, A., 2004. The complex architecture of oxygenic photosynthesis. Nat. Rev. Mol. Cell Biol. https://doi.org/10.1038/nrm1525.

Niyogi, K.K., Bjorkman, O., Grossman, A.R., 1997. The roles of specific xanthophylls in photoprotection. Proc.Natl.Acad.Sci.U.S.A 94, 14162–14167.

Peers, G., Truong, T.B., Ostendorf, E., Busch, A., Elrad, D., Grossman, A.R., Hippler, M., Niyogi, K.K., 2009a. An ancient light-harvesting protein is critical for the regulation of algal photosynthesis. Nature 462, 518–521. https://doi.org/10.1038/nature08587.

Peers, G., Truong, T.B., Ostendorf, E., Busch, A., Elrad, D., Grossman, A.R., Hippler, M., Niyogi, K.K., 2009b. An ancient light-harvesting protein is critical for the regulation of algal photosynthesis. Nature 462, 518–521. https://doi.org/10.1038/nature08587.

Perozeni, F., Stella, G.R., Ballottari, M., 2018. LHCSR expression under HSP70/RBCS2 promoter as a strategy to increase productivity in microalgae. Int. J. Mol. Sci. https://doi.org/10.3390/ijms19010155.

Peter, G.F., Thornber, J.P., 1991. Electrophoretic procedures for fractionation of photosystem-I and photosystem-II pigment-proteins of Higher plants and for determination of their subunit composition (A c. di). In: Rogers, L.J. (Ed.), Methods in Plant Biochemistry. 5. Academic Press, New York, pp. 195–210.

Pinnola, A., Cazzaniga, S., Alboresi, A., Nevo, R., Levin-Zaidman, S., Reich, Z., Bassi, R., 2015a. Light-harvesting complex stress-related proteins catalyze excess energy dissipation in both photosystems of *Physcomitrella patens*. Plant Cell. https://doi.org/10.1105/tpc.15.00443.

Pinnola, A., Ghin, L., Gecchele, E., Merlin, M., Alboresi, A., Avesani, L., Pezzotti, M., Capaldi, S., Cazzaniga, S., Bassi, R., 2015b. Heterologous expression of moss light-harvesting complex stress-related 1(LHCSR1), the chlorophyll *A*-xanthophyll pigment-protein complex catalyzing non-photochemical quenching, in Nicotiana sp. J. Biol. Chem. 290, 24340–24354. https://doi.org/10.1074/jbc.M115.668798.

Redekop, P., Rothhausen, Natalie, Rothhausen, Natascha, Melzer, M., Mosebach, L., Dülger, E., Bovdilova, A., Caffarri, S., Hippler, M., Jahns, P., 2020. PsbS contributes to photoprotection in Chlamydomonas reinhardtii independently of energy dissipation. Biochim. Biophys. Acta - Bioenerg. https://doi.org/10.1016/j.bbabio.2020.148183.

Rodolfi, L., Zittelli, G.C., Bassi, N., Padovani, G., Biondi, N., Bonini, G., Tredici, M.R., 2009. Microalgae for oil: strain selection, induction of lipid synthesis and outdoor mass cultivation in a low-cost photobioreactor. Biotechnol. Bioeng. 102, 100–112. https://doi.org/10.1002/bit.22033.

Ruban, A.V., Johnson, M.P., Duffy, C.D.P., 2012. The photoprotective molecular switch in the photosystem II antenna. Biochim. Biophys. Acta - Bioenerg. https://doi.org/10.1016/j.bbabio.2011.04.007.

Scott, S.A., Davey, M.P., Dennis, J.S., Horst, I., Howe, C.J., Lea-Smith, D.J., Smith, A.G., 2010. Biodiesel from algae: challenges and prospects. Curr. Opin. Biotechnol. https://doi.org/10.1016/j.copbio.2010.03.005.

Stephenson, P.G., Moore, C.M., Terry, M.J., Zubkov, M.V., Bibby, T.S., 2011. Improving photosynthesis for algal biofuels: toward a green revolution. Trends Biotechnol. 29, 615–623. https://doi.org/10.1016/j.tibtech.2011.06.005.

Sueoka, N., 1960. Mitotic replication of Deoxyribonucleic acid in Chlamydomonas reinhardi. Proc. Natl. Acad. Sci. https://doi.org/10.1073/pnas.46.1.83.

Towbin, H., Staehelin, T., Gordon, J., 1979. Electrophoretic transfer of proteins from polyacrylamide gels to nitrocellulose sheets: procedure and some applications. Proc. Natl. Acad. Sci. U. S. A. https://doi.org/10.1073/pnas.76.9.4350.

Truong, A., 2011. Title Investigating the Role(s) of LHCSRs in Chlamydomonas reinhardtii.

Van Amerongen, H., Croce, R., 2013. Light harvesting in photosystem II. Photosynth. Res. https://doi.org/10.1007/s11120-013-9824-3.

Van Kooten, O., Snel, J.F.H., 1990. The use of chlorophyll fluorescence nomenclature in plant stress physiology. Photosynt.Res. 25, 147–150. _ _.

Vecchi, V., Barera, S., Bassi, R., Dall'osto, L., 2020. Potential and challenges of improving photosynthesis in algae. Plants 9. https://doi.org/10.3390/plants9010067.

Weyer, K.M., Bush, D.R., Darzins, A., Willson, B.D., 2010. Theoretical maximum algal oil production. Bioenergy Res. 3, 204–213. https://doi.org/10.1007/s12155-009-9046-x.

Zhu, X.-G., Long, S.P., Ort, D.R., 2010. Improving photosynthetic efficiency for greater yield. Annu. Rev. Plant Biol. 61, 235–261. https://doi.org/10.1146/annurev-arplant-042809-112206.